frontiers | Frontiers in Energy Research

BRIEF RESEARCH REPORT
published: 22 July 2022
doi: 10.3389/fenrg.2022.950521

Optimal Configuration of Fire-Storage Capacity Considering Dynamic Charge-Discharge Efficiency of Hybrid Energy Storage

Hongbo Huang*, Hui Wang, Yang Cai, Xiwei Chen and Tingting Li

Powerchina Hubei Electric Engineering Co., Ltd, Wuhan, China

The combination of thermal power and hybrid energy storage is an effective way to improve the response ability of automatic generation control (AGC) command in thermal power plants. Notably, the configuration of hybrid energy storage capacity is directly related to improvement of the frequency modulation ability of thermal power plants and the coordination of economic benefits. However, the constant efficiency model adopted in capacity configuration will misjudge the actual operating status of each energy storage unit, resulting in unreasonable capacity allocation. In this context, a fire-storage capacity optimization configuration model considering the dynamic charge–discharge efficiency of hybrid energy storage is established. The model presents the functional relationship between charge and discharge power and the efficiency of different types of energy storage. Simulation proves that the proposed strategy can meet the tracking demand of area control error signal in thermal power plants and reduce the planning and operation cost of energy storage.

Keywords: energy storage-thermal power combination, AGC response, hybrid energy storage system, capacity configuration, dynamic efficiency

OPEN ACCESS

Edited by:
Xun Shen,
Tokyo Institute of Technology, Japan

Reviewed by:
Sandeep Kumar Duran,
Lovely Professional University, India
Gaurav Sachdeva,
DAV University, India

****Correspondence:***
Hongbo Huang
x997050035@163.com

Specialty section:
This article was submitted to Smart Grids,
a section of the journal Frontiers in Energy Research

Received: *23 May 2022*
Accepted: *13 June 2022*
Published: *22 July 2022*

Citation:
Huang H, Wang H, Cai Y, Chen X and Li T (2022) Optimal Configuration of Fire-Storage Capacity Considering Dynamic Charge-Discharge Efficiency of Hybrid Energy Storage. Front. Energy Res. 10:950521. doi: 10.3389/fenrg.2022.950521

1 INTRODUCTION

In China, thermal power plants mainly undertake secondary frequency modulation auxiliary services (Jin et al., 2022): adjusting unit output in real time according to automatic generation control (AGC) instructions. In recent years, with the reform of China's energy structure, the complexity of system AGC instruction characteristics has increased (Sun et al., 2020; Yang et al., 2021; Yang et al., 2022). In this context, the problems of long inherent response delay and low climbing rate of traditional thermal power units (Zhang et al., 2018; Zhang et al., 2021) will increase the tracking error of AGC instructions and make it difficult to ensure the safety of power grid frequency. Energy storage, as a new type of frequency modulation resource, has the characteristics of fast response, accurate control, and two-way output (Meng et al., 2019), which can assist the thermal power plant in instantly tracking power instructions. Therefore, the configuration of a certain capacity energy storage system in a thermal power plant is an effective method to solve the AGC response problem of the whole plant.

There are various types of energy storage inside the hybrid energy storage, which can meet the energy density and power density requirements of frequency modulation instructions. Therefore, compared with single energy storage, hybrid energy storage can greatly improve the AGC response capacity of thermal power plants (Ye et al., 2021; Saxena and Shankar, 2022) and effectively improve the stability and economy of energy storage combination plants. However, the capacity configuration cost of the hybrid energy storage system is contradictory to the improvement of AGC response capability of the whole plant: too much energy storage capacity configuration will lead to increase of energy storage operation planning cost, and too little configuration will lead to failure to compensate for the poor AGC response capability of thermal power units. Therefore, in order to improve the response capacity of AGC of thermal power plants and ensure the economy of energy storage system planning and operation, optimizing the configuration of hybrid energy storage capacity is an important link for energy storage to participate in the large-scale development of AGC response of thermal power plants.

The objectives of the capacity configuration of the AGC frequency modulation hybrid energy storage system for auxiliary thermal power units include the following: 1) improvement in AGC response performance of the whole plant; 2) reduction in the planning and operation cost of the hybrid energy storage system. In order to achieve this goal, it is necessary to allocate the power in the AGC frequency modulation responsibility signal of the energy storage system to different energy storage units so as to give full play to the technical advantages of different energy storage media in the hybrid energy storage system to meet the coordination of economy and regulation of the whole plant.

Yang (2016), Liu et al. (2021), and Meng et al. (2021) set the power distribution strategy of hybrid energy storage based on the decomposition of the Area Control Error (ACE) signal in the frequency domain and carried out capacity optimization on this basis. However, the control cycle of secondary frequency modulation is more than 1 min, and the response time of different types of energy storage devices is within 5 s, so the difference between different response characteristics can be ignored. Therefore, this method is not applicable to the power distribution of hybrid energy storage oriented to AGC of thermal power plants. Wang et al. (2018); Aghajan-Eshkevari et al. (2022) adopt the “priority” allocation method to carry out capacity configuration, such as preferential charging and discharging power allocation method for supercapacitors.

In this way, according to the analysis of the operation mechanism of some auxiliary service markets, the general rule of maximizing profits is obtained, and then the output priority level of each energy storage type is formulated according to the rule, which is more suitable for some specific scenarios. However, this method is subjective and poor in scalability. In the studies by Cheng et al. (2014) and Galatsopoulos et al. (2020), dynamic optimization of the ACE signal allocation ratio is considered in capacity configuration so as to give full play to the frequency modulation potential of different types of energy storage in various scenarios. In the abovementioned study, the charge and discharge efficiency of each type of energy storage is regarded as a constant. In fact, the efficiency of charge and discharge changes dynamically with the distribution of power. Ignoring the dynamic characteristics of charging and discharging efficiency will lead to unreasonable allocation of energy storage capacity and affect the frequency modulation performance and configuration cost of hybrid energy storage. In this regard, the charge–discharge power-efficiency model of the battery energy storage unit was established (Rancilio et al., 2019), but only the dynamic characteristics of the charge–discharge efficiency of a single type of energy storage were considered. Iclodean et al. (2017) discuss the dynamic characteristics of charge and discharge efficiency of compressed air energy storage and electrochemical energy storage, but it is only described by a simple model in the form of a segmented function, which is different from the dynamic model of actual power-charge and discharge efficiency. Furthermore, the previously mentioned pieces of literature did not consider the optimal allocation of capacity.

To sum up, this study adopts a hybrid energy storage system comprising batteries and supercapacitors to assist traditional thermal power plants in providing AGC auxiliary services. Aiming at the capacity configuration problem of the hybrid energy storage system, this study establishes a refinement dynamic model of charging and discharging power efficiency of each type of energy storage unit. Based on this, a fire-storage capacity configuration model considering the dynamic charge–discharge efficiency of hybrid energy storage is constructed to dynamically optimize the proportion of ACE signal allocation so as to obtain the rated energy storage capacity that meets the requirement of instruction tracking and minimizes the cost of energy storage planning and operation. Finally, the superiority and economy of the proposed strategy are verified by simulation.

2 THE DYNAMIC EFFICIENCY MODEL OF HYBRID ENERGY STORAGE CHARGE–DISCHARGE POWER

2.1 Dynamic Efficiency Model of Battery

When the battery participates in AGC frequency modulation in a thermal power plant, the incoming power can be changed by adjusting the charge and discharge current of the internal circuit so that it can meet the requirements of auxiliary frequency modulation power. With the dynamic change of charge and discharge current, the battery terminal voltage will also change, so the charge and discharge efficiency determined by the terminal voltage too will change. The mathematical model of dynamic charging and discharging efficiency of the previously mentioned batteries is as follows:

$$P_i^b = U_i^b I_i^b = \left(E_i^b - I_i^b R_i^b\right) I_i^b \tag{1}$$

$$\eta_{i,t}^b = \begin{cases} \dfrac{U_{i,t}^b}{E_i^{\mathrm{b}}} = \dfrac{E_i^b - I_{i,t}^b R_{i,t}^b}{E_i^{\mathrm{b}}}, I_{i,t}^b \geq 0 \\ \dfrac{E_i^b}{U_{i,t}^b} = \dfrac{E_i^b}{E_i^b + I_{i,t}^b R_{i,t}^b}, I_{i,t}^b < 0 \end{cases} \tag{2}$$

In the formula, R_i^b and E_i^b are equivalent internal resistance and open circuit potential of battery i respectively; $U_{i,t}^b$, $I_{i,t}^b$, $\eta_{i,t}^b$, and P_i^b are the terminal voltage, charge and discharge current, charge and discharge efficiency, and charge and discharge power of battery i at time t (positive for discharge and negative for charge), respectively.

The SOC status of the battery is as follows:

$$S_{i,t}^{b}\eta_{i,t}^{b} = S_{i,t-1}^{b}\eta_{i,t-1}^{b} - \frac{P_{i,t}^{b}\Delta t}{C_{i}^{b}}. \tag{3}$$

In the formula, $S_{i,t}^{b}$ is the SOC state value of battery i at time t. During operation, $S_{i,t}^{b}$ should meet the constraints shown in the equation. C_{i}^{b} is the rated capacity of battery i.

$$S_{i}^{b,\min} \le S_{i,t}^{b} \le S_{i}^{b,\max} \tag{4}$$

In the formula, $S_{i}^{b,\max}$ and $S_{i}^{b,\min}$ are the maximum and minimum SOC values of battery I ,respectively.

2.2 Dynamic Efficiency Model of a Supercapacitor

In this study, the current loop of the supercapacitor adopts a constant power control mode, and the series structure of ideal capacitance and equivalent series internal resistance is used to simulate the internal circuit of the supercapacitor (Naseri et al., 2021). Unlike batteries, the charging and discharging efficiency of supercapacitors is related only to power.

$$\eta_{i,t}^{s} = \begin{cases} 1 + \dfrac{2R_{i}^{S}\ln d_{i}}{U_{s,i}^{\max}\left(1-d_{i}^{2}\right)}P_{i,t}^{s}, P_{i,t}^{s} \ge 0 \\ \dfrac{1}{1 - \dfrac{2R_{i}^{S}\ln d_{i}}{U_{s,i}^{\max}\left(1-d_{i}^{2}\right)}P_{i,t}^{s}}, P_{i,t}^{s} < 0 \end{cases} \tag{5}$$

In the formula, R_{i}^{S}, $U_{s,i}^{\max}$, and d_{i} are the equivalent resistance of supercapacitor I, the maximum voltage, and discharge factor of ideal capacitor i ,respectively; $P_{i,t}^{s}$ and $\eta_{i,t}^{s}$ are, respectively, the charge–discharge power and charge–discharge efficiency of supercapacitor i at time t (discharge is positive and charge is negative).

The SOC of the supercapacitor is as follows:

$$S_{i,t}^{s}\eta_{i,t}^{s} = S_{i,t-1}^{s}\eta_{i,t-1}^{s} - \frac{P_{i,t}^{s}\Delta t}{\eta_{i,t}^{s}C_{i}^{s}} \tag{6}$$

In the formula, $S_{i,t}^{s}$ is the SOC state value of supercapacitor i at time t. During operation, $S_{i,t}^{b}$ should meet the constraints shown in the formula. C_{i}^{s} is the rated capacity of supercapacitor i.

$$S_{i}^{s,\min} \le S_{i,t}^{s} \le S_{i}^{s,\max} \tag{7}$$

In the formula, $S_{i}^{s,\min}$ and $S_{i}^{s,\max}$ are the maximum and minimum SOC values of supercapacitor I, respectively.

2.3 Importance Analysis of the Dynamic Efficiency Model of the Energy Storage Unit

In order to analyze the importance of dynamic efficiency of the energy storage unit to capacity allocation, the electric quantity fluctuation range $\Delta E_{i,t}$ is introduced as follows:

$$\Delta E_{i,t}^{b} = C_{i}^{b}\left|S_{i,t}^{b} - S_{i,t-1}^{b}\right| = \begin{cases} \dfrac{P_{i,t}^{b}\Delta t}{\eta_{i,t}^{b}}, P_{i,t}^{b} \ge 0 \\ -\dfrac{P_{i,t}^{b}\Delta t}{\eta_{i,t}^{b}}, P_{i,t}^{b} < 0 \end{cases}. \tag{8}$$

$$\Delta E_{i,t}^{s} = C_{i}^{s}\left|S_{i,t}^{s} - S_{i,t-1}^{s}\right| = \begin{cases} \dfrac{P_{i,t}^{s}\Delta t}{\eta_{i,t}^{s}}, P_{i,t}^{s} \ge 0 \\ -\dfrac{P_{i,t}^{s}\Delta t}{\eta_{i,t}^{s}}, P_{i,t}^{s} < 0 \end{cases} \tag{9}$$

In the formula, $\Delta E_{i,t}^{b}/\Delta E_{i,t}^{s}$ represents the electric quantity fluctuation range of the battery/supercapacitor between $t-1$ and t. Under the same power curve and the smaller $\Delta E_{i,t}$ at each moment, the smaller the capacity requirement C_{i} to meet SOC constraints.

According to **Figure 1**, different from the constant state of charge and discharge efficiency in the configuration of energy storage capacity at that time, the actual charge and discharge power of the supercapacitor and battery changes dynamically with the power and is inversely proportional to the charge and discharge power. According to the numerical comparison between constant charge and discharge efficiency and dynamic charge and discharge efficiency, the charge and discharge power of each energy storage unit is segmented according to **Table 1**.

3 HYBRID ENERGY STORAGE CAPACITY ALLOCATION POLICY

After the hybrid energy storage system is configured in the thermal power plant, the AGC-responsive hybrid energy storage capacity configuration strategy is shown in **Figure 2**. In **Figure 2**, P^{ref} depicts the ACE signal transmitted by the AGC dispatching center to a thermal power plant, P^{m} is the real-time output of the conventional units in the thermal power plant jointly responding to the ACE signal, and the ACE signal tracking error P_{ref}^{s-b} caused by the inherent AGC response weakness of the traditional units is fully compensated by the hybrid energy storage system.

The key to the hybrid energy storage capacity configuration strategy is to propose a hybrid energy storage capacity configuration model to reduce the AGC response cost of hybrid energy storage on the premise of ensuring P_{ref}^{s-b} is fully compensated. At the same time, aiming at the nonlinear constraint and nonlinear objective function of the model, the linearization process is carried out by the BIG-M method and product type decomposition method so as to realize the optimal distribution of P_{ref}^{s-b} within the energy storage cluster and obtain the economic allocation of the capacity of each energy storage unit.

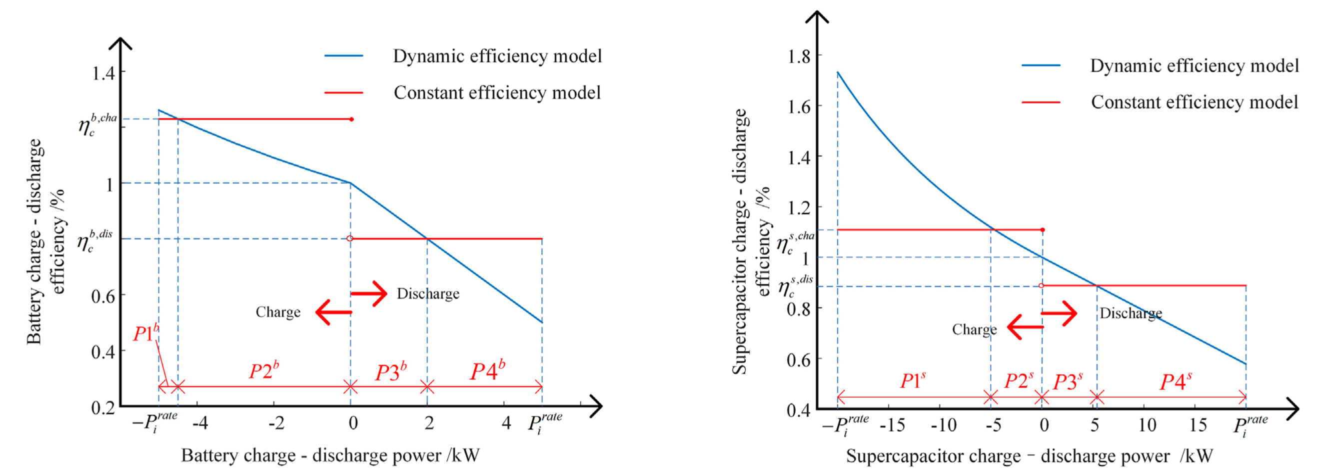

FIGURE 1 | Dynamic/constant efficiency curve of the energy storage unit with power.

3.1 Construction of the Hybrid Energy Storage Capacity Configuration Model

3.1.1 The Optimization Objective

The objective of the hybrid energy storage capacity configuration model is to minimize the total planning and operation cost F of the hybrid energy storage. F includes the fixed investment C^e of the capacity of each energy storage unit, the maintenance cost C^w of the machine, and the cost C^p of running electricity loss.

$$C^e = \sum_{i=1}^{E1} k_i^{e,b} C_i^b + \sum_{j=1}^{E2} k_j^{e,s} C_j^s \tag{10}$$

$$k_i^{e,b} = \frac{c_i^{e,b}\left(1+r_i^b\right)^{N_i^b}}{365\left[r_i^b\left(1+r_i^b\right)^{N_i^b}-1\right]} \tag{11}$$

$$k_j^{e,s} = \frac{c_j^{e,s}\left(1+r_j^s\right)^{N_j^s}}{365\left[r_j^s\left(1+r_j^s\right)^{N_j^s}-1\right]} \tag{12}$$

$$C^w = \sum_{i=1}^{E1} \frac{c_i^{w,b} C_i^b}{365} + \sum_{j=1}^{E2} \frac{c_j^{w,s} C_j^s}{365}. \tag{13}$$

TABLE 1 | Charge and discharge power segmentation basis.

Power of charge and discharge segments	Judgement method
$P1^s$, $P1^b$	Dynamic charging efficiency ≥ Constant charging efficiency
$P2^s$, $P2^b$	Dynamic charging efficiency < Constant charging efficiency
$P3^s$, $P3^b$	Dynamic discharge efficiency ≥ Constant discharge efficiency
$P4^s$, $P4^b$	Dynamic discharge efficiency < Constant discharge efficiency

$$C^p = \sum_{t=1}^{17280}\left[\sum_{i=1}^{E1} c_i^{p,b}\cdot P_{i,t}^b\left(\frac{1}{\eta_{i,t}^b}-1\right) + \sum_{j=1}^{E2} c_j^{p,s}\cdot P_{j,t}^s\left(\frac{1}{\eta_{j,t}^s}-1\right)\right] \tag{14}$$

In the formula,$c_i^{e,b}$ and $c_j^{e,s}$ are the investment cost coefficients of battery I and supercapacitor j per unit capacity, respectively; $c_i^{w,b}$ and $c_j^{p,s}$ are maintenance cost coefficients of battery i and supercapacitor j per unit electric quantity, respectively; $c_i^{p,b}$ and $c_j^{p,s}$ are the cost coefficients of battery i and supercapacitor j (unit price of online connection), respectively. r_i^b and r_j^s are the discount rates of battery i and supercapacitor j; N_i^b and N_j^s are the floating charge life of battery i and supercapacitor j.

Since the capacity unit price of the power energy storage unit is much higher than that of the capacity energy storage unit as well as the maintenance cost and Internet access unit price of each unit, the fixed investment of the capacity of the power energy storage unit becomes the main cost of the hybrid energy storage system. Therefore, reducing the capacity configuration of the power energy storage unit can effectively improve the economy of the hybrid energy storage system.

3.1.2 Constraint Conditions

In addition to **Eqs 1–7**, the constraint conditions of the fire-storage capacity configuration model also includes power balance constraint 15, charge–discharge power constraint 16–17, climbing constraint 18–19, current constraint 20, and charge–discharge efficiency constraint 21–22.

$$P_{ref,t}^{s-b} = \sum_{i=1}^{E1} P_{i,t}^b + \sum_{j=1}^{E2} P_{j,t}^s. \tag{15}$$

$$-P_i^{b,rate} \le P_{i,t}^b \le P_i^{b,rate}. \tag{16}$$

$$-P_i^{s,rate} \le P_{i,t}^s \le P_i^{s,rate}. \tag{17}$$

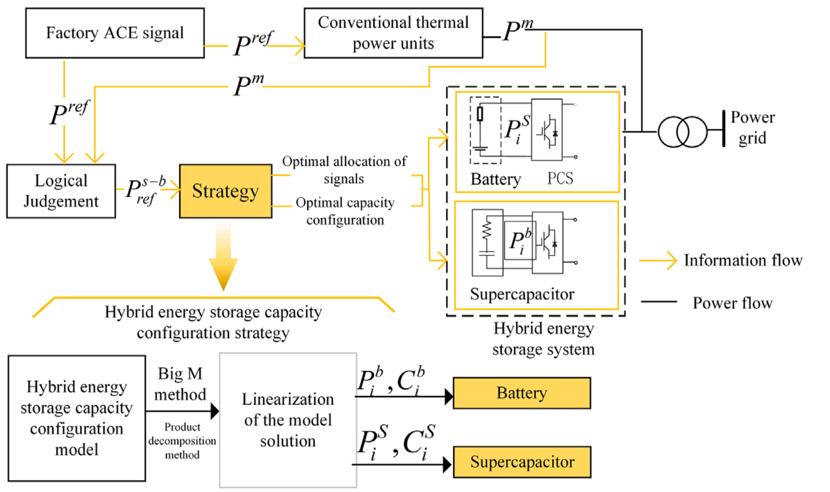

FIGURE 2 | Hybrid energy storage capacity configuration strategy.

TABLE 2 | Classification of non-convex terms for the model.

Category	Characteristics	Correspondence	Log-linear
1	$z = \frac{x}{y}$	(14)	*Continuousiterativealgorithm* (Song et al., 2018)
2	$z = xy$	(1)	*Continuousiterativealgorithm* (Song et al., 2018)
3	$z = \frac{1}{1+k1*x}$	(2) (5)	*Continuousiterativealgorithm*
4	$z = \begin{cases} x, if y \geq 0 \\ p, if y \leq 0 \end{cases}$	(2) (5)	*BigMmethod* (Anderson-Cook and Robinson, 2009)
5	$z = \lvert x \rvert$		*BigMmethod* (Anderson-Cook and Robinson, 2009)

In this Table, x, y, z, p are variables.

$$-R_i^{b,dn} \leq P_{i,t}^b - P_{i,t-1}^b \leq R_i^{b,up}. \tag{18}$$

$$-R_i^{s,dn} \leq P_{i,t}^s - P_{i,t-1}^s \leq R_i^{s,up}. \tag{19}$$

$$-I_i^{b,rate} \leq I_{i,t}^b \leq I_i^{b,rate} \tag{20}$$

$$\eta_i^{b,\min} \leq \eta_{i,t}^b \leq \eta_i^{b,\max}. \tag{21}$$

$$\eta_i^{s,\min} \leq \eta_{i,t}^s \leq \eta_i^{s,\max}. \tag{22}$$

In the formula stated above, $P_{i,t}^{ref}$ is the incoming power of energy storage unit i at time t; the number of units of $E1$ and $E2$ battery cluster and supercapacitor cluster is the number of units of the hybrid energy storage system. $P_i^{b,rate}$ and $P_i^{s,rate}$ are the rated power of battery i and supercapacitor i, respectively; $R_i^{s,up}$ and $R_i^{b,dn}$ demonstrate the ascending and descending climbing rates of supercapacitor i respectively. $I_i^{b,rate}$ is the rated current of battery i; $\eta_i^{b,\max}$ and $\eta_i^{b,\min}$ are the maximum and minimum charge and discharge efficiency of battery i, respectively. $\eta_i^{s,\max}$ and $\eta_i^{s,\min}$ are the maximum and minimum charge and discharge efficiency of supercapacitor i, respectively.

3.2 Model Processing and Solution

3.2.1 Model Linearization

The configuration model of hybrid energy storage capacity has five types of non-convex terms as shown in **Table 2**, resulting in increased difficulty in optimization. In this regard, this study adopts different linearization methods for these five types of non-convex terms, as shown in **Table 2** below:

3.2.2 Model Solving

According to the abovementioned linearization method, the solution process of the hybrid energy storage capacity configuration model considering the dynamic charging–discharge efficiency model is shown in **Figure 3**.

4 EXAMPLE ANALYSIS

This study takes a thermal power plant with a hybrid energy storage system consisting of batteries and supercapacitors as a simulation example. The total output and ACE signal of the whole plant without energy storage on a certain day are selected, and the parameters of the hybrid energy storage system are shown in **Table 3**. Considering the actual operating conditions of the project-SOC differences among energy storage units, each energy

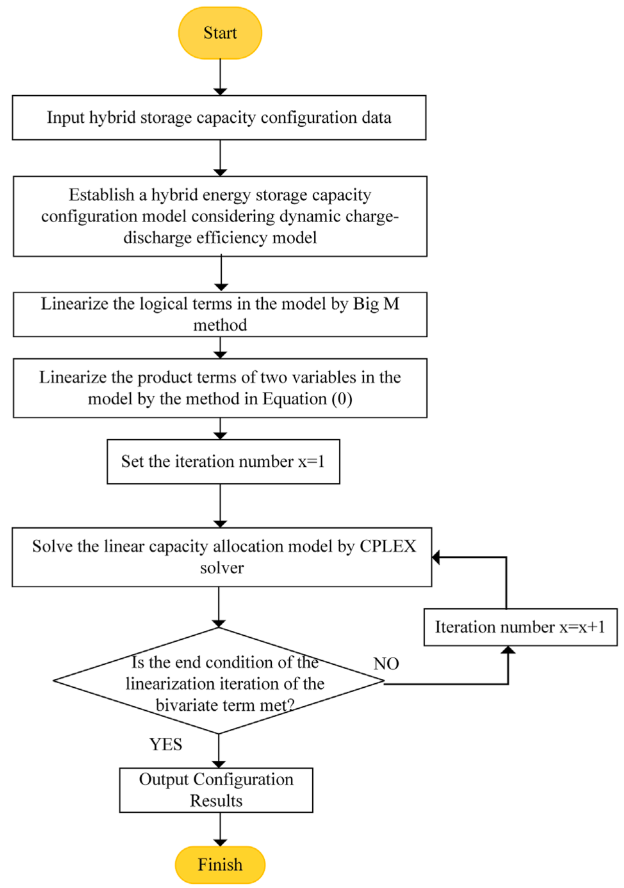

FIGURE 3 | Solution process.

TABLE 3 | Unit parameters.

Index	Battery	Supercapacitor
R^b/Ω	7.8	–
$E^b/V\Omega$	60	–
U_E^{max}/V	–	70
U_E^{max}/V	–	70
R^S/Ω	–	2.8
P^{rate}/kW	10	20
$c^l/(\$/kW.h)$	2,000	1,500
$c^e/(\$/kW.h)$	2,000	1,500
$c^e/(\$/kW.h)$	640	27,000
$c^w/(\$/kW.h)$	0.05	0.05
$c^p/(\$/kW.h)$	1	1
r	0.08	0.08
N/a	4	20
η_{PCS}^{inv}	0.85	0.85
η_{PCS}^{conv}	0.85	0.85
S_{max}	0.8	0.9
S_{min}	0.2	0.1
$R^{up}/(kW/s)$	20	2,000
$R^{dn}/(kW/s)$	20	2,000

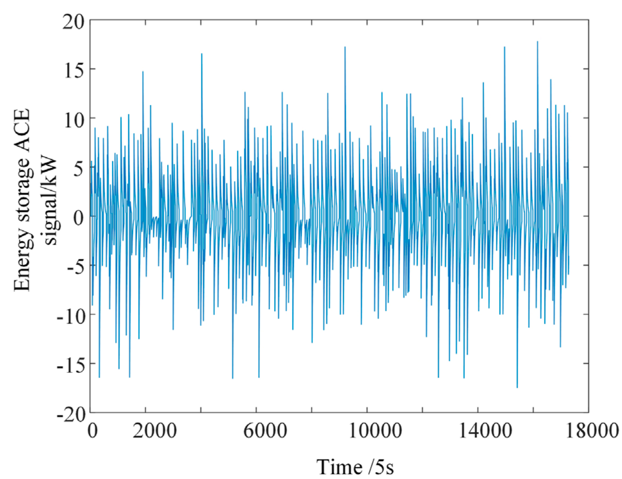

FIGURE 4 | Hybrid energy storage system's P_{ref}^{s-b} .

storage unit is set to have SOC differences, and the initial SOC of the battery and supercapacitor is 0.4 and 0.5, respectively. The model was built and solved on MATLAB 2018b platform using YALMIP toolbox and GUROBI9.1.2 solver on a computer configured with Win10 system, AMD R7-5800H processor, and 16G RAM.

The common full compensation strategy in power plant energy storage engineering introduced by the energy storage demonstration project of Shijingshan Power Plant, which has been practiced online, is adopted: energy storage complete compensation for the difference between real-time monitoring AGC command and unit output data, namely, $P_{ref}^{s-b} = P^{ref} - P^{m}$. P_{ref}^{s-b} curve is shown in **Figure 4**, and the sampling period of the original data is $\Delta t = 5s$.

To verify the effectiveness and superiority of the strategies proposed in this study,the comparison strategies shown in **Table 4** is set.

4.1 Capacity Optimization Results

The purpose of capacity configuration is to ensure the frequency modulation effect of AGC and reduce the operation cost of energy storage planning. The capacity optimization results of different strategies are shown in **Table 5**. In energy storage output to P_{ref}^{s-b} command signal tracking error $\zeta_t(\zeta_t = \left|\sum_{i=1}^{M} P_{i,t} - P_{ref,t}^{s-b}\right|)$ to represent the AGC frequency modulation effect, the effect of different strategies of AGC response is shown in **Figure 5**. The actual operation of the energy storage system includes dynamic charge–discharge efficiency model and corresponding dynamic SOC constraints. The capacity of energy storage unit optimized by strategy 3 is put into the actual operation model of energy storage to obtain the actual value of strategy 3. The ideal value of strategy 3 is the result of direct optimization of the corresponding model of strategy 3.

According to the analysis of **Table 5** and **Figure 5**, the results are as follows:

TABLE 4 | Capacity optimization strategy comparison settings.

Capacity configuration strategy	Implication
Strategy 1	The strategy of this study: the hybrid energy Storage and dynamic charge–discharge Efficiency model
Strategy 2	Single energy storage and dynamic Charge–discharge efficiency model
Strategy 3	Hybrid energy storage and constant Charge–discharge efficiency model

TABLE 5 | Configuration results for different capacity optimization strategies.

Index	Strategy 1	Strategy 2	Strategy 3 – ideal value	Strategy 3 – actual value
$C^b/(kW.h)$	4,326.4	–	687.7	687.7
$C^S/(kW.h)$	1,762.4	5,007.1	839.9	839.9
$\sum_{i=1}^{M} F_i/(\$)$	13,548	32,293	5,766.7	5,765.8
Daily Average ζ_t	0	1	0	0.5

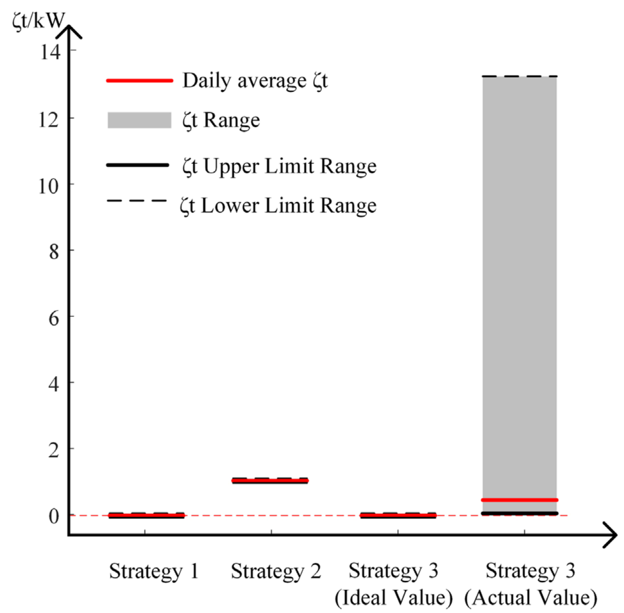

FIGURE 5 | AGC response effects for different strategies.

1) The operation planning cost of strategy 1 is lower than that of strategy 2. Furthermore, the daily average ζ_t (0 kW) and ζ_t lower limit (0 kW) of strategy 1 are less than the daily average ζ_t (1 kW) and ζ_t lower limit (1 kW) of Strategy 2. Therefore, compared with single energy storage, hybrid energy storage can reduce energy storage operation planning costs and tracking error ζ_t;

2) The operation planning cost calculated by the scheduling model of different strategies is the expected cost value. Among them, the expected cost of strategy 3 is $5766.7, less than the planned operating cost of strategy 1 which is $13,548. Taking the capacity optimization result of the dynamic charge–discharge model as the actual value, it can be seen that the capacity optimization strategy using the constant charge–discharge model is easy to cause investors to expect too low investment costs.

3) Under the actual dynamic charge–discharge model and SOC constraints, the actual output and charge–discharge efficiency of strategy 3 are all different from those of the optimized model. In strategy 3, the actual daily average ζ_t (0.5 kw) is higher than the minimum value (0 kw), and there exists the ζ_t margin. However, in strategy 3, without considering the actual dynamic charge–discharge efficiency, the actual daily average ζ_t judged by the optimization model of strategy 3 is the lowest value, and there is no ζ_t margin. Therefore, the capacity optimization strategy of the constant charging–discharge model will lead to low prediction of tracking error of P_{ref}^{s-b} instruction signal by the operator.

(4) The daily average ζ_t of strategy 1 is the minimum, and there is no ζ_t margin. Therefore, the capacity optimization strategy of the dynamic charge–discharge model can improve the utilization rate of the energy storage system, fully compensate the P_{ref}^{s-b} command signal, and guarantee the AGC frequency modulation effect of the whole plant.

4.2 Analysis of Capacity Optimization Results

The output comparison of each energy storage unit under strategy 1 and Strategy 3 (ideal) is shown in **Figure 6**. It can be seen that the output results of the unit under the capacity optimization strategy of the constant charge–discharge efficiency model and the capacity optimization strategy of the dynamic charge–discharge efficiency model are similar. At this point, under the same output situation, the capacity configuration of the dynamic charge–discharge efficiency model and the constant charge–discharge efficiency model

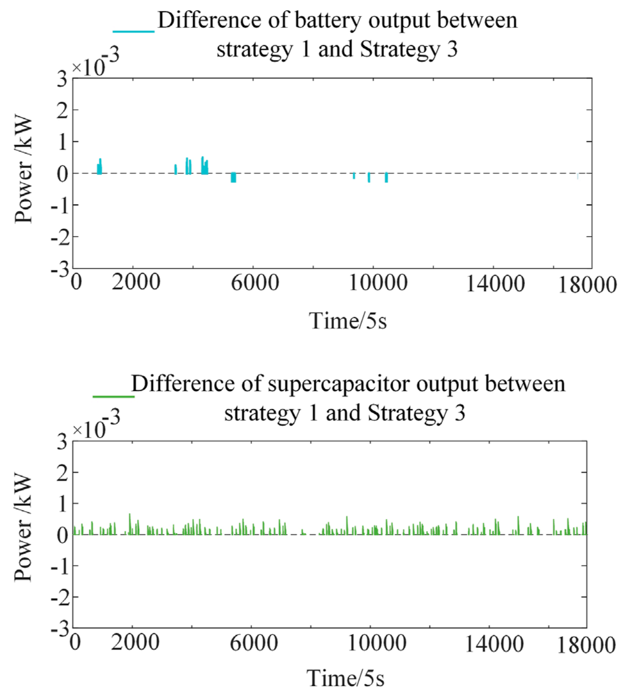

FIGURE 6 | Comparison of energy storage output between strategy 1 and strategy 3.

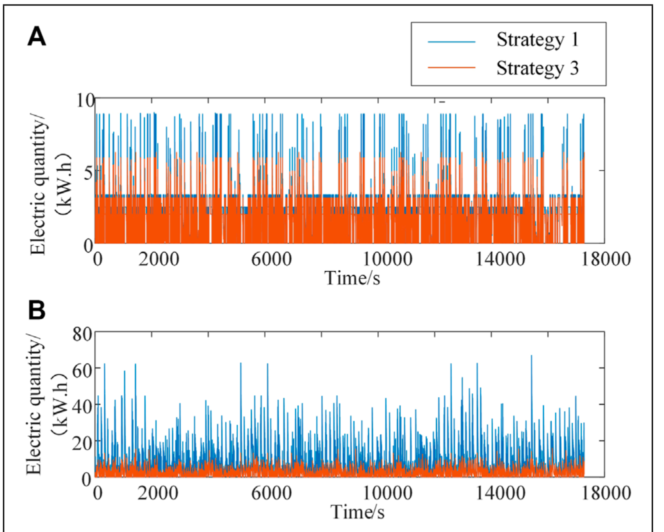

FIGURE 7 | Strategy 1/3's ΔE **(A)** Variation range of battery electric quantity per unit time.**(B)**Variation range of supercapacitor electric quantity per unit time.

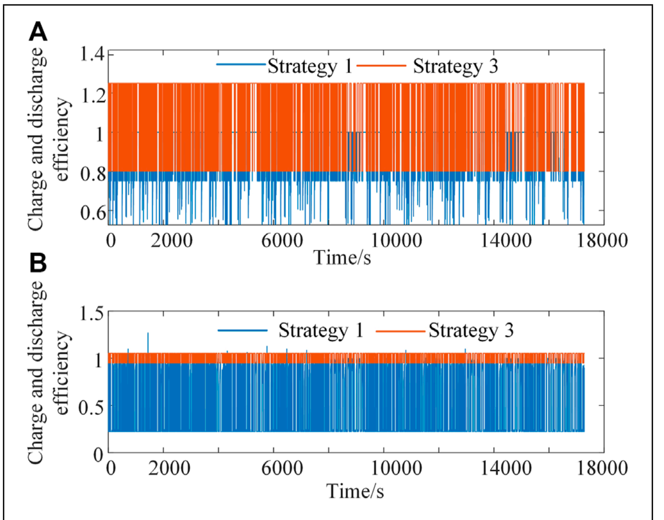

FIGURE 8 | Charge–discharge efficiency of strategy 1 and strategy 3. **(A)** Charge and discharge efficiency of battery. **(B)** Charge and discharge efficiency of supercapacitor.

is mainly influenced by the comparison of the amount of electric quantity $\Delta E^{s}_{i,t-1\rightarrow t}$ increased (or lost) per unit time, which depends on the charge–discharge efficiency of the two models.

Figure 7 shows the ΔE curves of Strategy 1 and Strategy 3 (ideal). As the charge–discharge efficiency of strategy 1 is lower than that of strategy 3 (ideal) in most time periods (as shown in **Figure 7**), ΔE of strategy 1 is higher than ΔE of Strategy 3 (ideal). In order to meet the SOC constraints of energy storage units, the capacity configuration of strategy 1 is higher than that of strategy 3 (as shown in **Table 5**).

As shown in **Figure 8**, considering the dynamic charge–discharge efficiency model, under the capacity configuration and power allocation of strategy 1 and Strategy 3 (ideal), the SOC curve of strategy 1 or strategy 3 is shown in **Figure 9**. It can be seen that the capacity configuration under the constant charge–discharge efficiency model makes the energy storage system over-charge and over-discharge, and the energy storage system will exit the AGC response in some period of time, resulting in the tracking error of P^{s-b}_{ref} command signal and reducing the AGC response performance of the energy storage.

However, the dynamic charge–discharge efficiency model, due to the appropriately expanded capacity configuration, makes the SOC state of each energy storage unit within the constraint range, meets the continuity requirements of P^{s-b}_{ref} command signal tracking, and improves the AGC response performance of energy storage.

To sum up, the strategy in this study takes into account the dynamic charge–discharge efficiency model and combines the characteristics of each energy storage unit to economically distribute P^{s-b}_{ref} instruction signals. At the same time, compared with the constant charge–discharge efficiency model, the strategy in this study can sense the charge–discharge efficiency conforming to the actual situation, rationally allocate the energy storage capacity, meet the continuity requirements of P^{s-b}_{ref} command signal tracking under the condition of considering SOC constraints, and improve the AGC response performance of the energy storage.

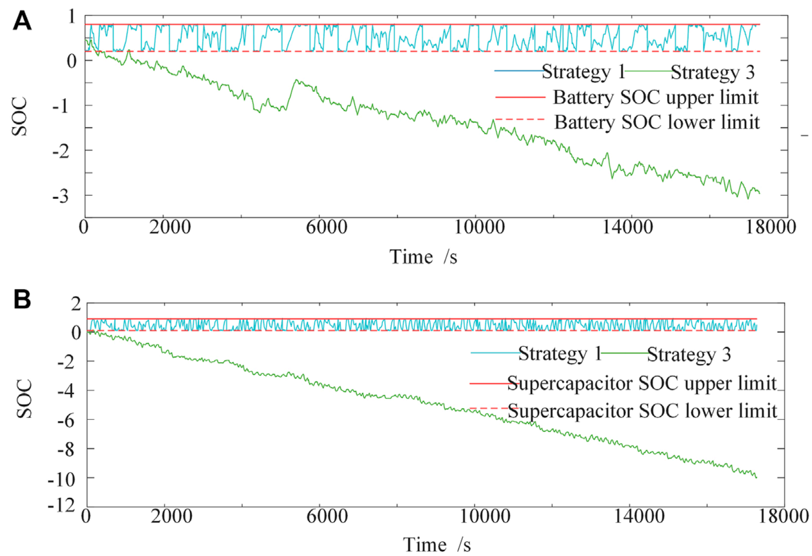

FIGURE 9 | SOC for strategy 1 and strategy 3 **(A)** Battery SOC. **(B)** Supercapacitor SOC.

5 CONCLUSION

The combined AGC response of hybrid energy storage and thermal power unit is an effective way to improve the AGC command tracking demand of thermal power plants. In this study, a fine dynamic model of charging and discharging power-efficiency of storage battery and supercapacitor is established. On this basis, the fire-storage capacity configuration model is established, which is used to realize the corresponding capacity configuration to meet the requirements of ACE signal tracking in thermal power plants and the minimum planning and operation cost of the energy storage system. The results of examples state that

1) The dynamic charge–discharge efficiency model can avoid over-charge and over-discharge of units, improve the energy storage availability, completely compensate for the ACE signal tracking error caused by the inherent AGC response disadvantage of conventional units, and improve the AGC response performance of thermal power plants;

2) The use of the constant charge–discharge efficiency model will lead to low investment cost expectations of investors, while the dynamic charge–discharge efficiency model can more accurately evaluate the operation planning cost of hybrid energy storage.

DATA AVAILABILITY STATEMENT

The raw data supporting the conclusions of this article will be made available by the authors, without undue reservation.

AUTHOR CONTRIBUTIONS

HH determined the direction and main points of the research, HH and HW proposed the technical route of the research, HH and YC completed the writing of the research content, YC, and XC completed the simulation verification of the numerical example, and TL revised the grammar and sentence structure of the study.

FUNDING

This manuscript was supported in part by the Science and Technology Project of Hubei Electric Power Survey and Design Institute K2020-2-06.

REFERENCES

Aghajan-Eshkevari, S., Azad, S., Nazari-Heris, M., Ameli, M. T., and Asadi, S. (2022). Charging and Discharging of Electric Vehicles in Power Systems: An Updated and Detailed Review of Methods, Control Structures, Objectives, and Optimization Methodologies. *Sustainability* 14 (4), 2137. doi:10.3390/su14042137

Anderson-Cook, C. M., and Robinson, T. J. (2009). A Designed Screening Study with Prespecified Combinations of Factor Settings. *Qual. Eng.* 21 (4), 392. doi:10.1080/08982110903179069

Cheng, Y., Tabrizi, M., Sahni, M., Povedano, A., and Nichols, D. (2014). Dynamic Available Agc Based Approach for Enhancing Utility Scale Energy Storage Performance. *IEEE Trans. Smart Grid* 5 (2), 1070–1078. doi:10.1109/tsg.2013.2289380

Galatsopoulos, C., Papadopoulou, S., Ziogou, C., Trigkas, D., and Voutetakis, S. (2020). Optimal Operation of a Residential Battery Energy Storage System in a Time-Of-Use Pricing Environment. *Appl. Sci.* 10 (17), 5997. doi:10.3390/app10175997

Iclodean, C., Varga, B., Burnete, N., Cimerdean, D., and Jurchiş, B. (2017). Comparison of Different Battery Types for Electric Vehicles. *IOP Conf. Ser. Mat. Sci. Eng.* 252, 012058. doi:10.1088/1757-899x/252/1/012058

Jin, L., He, L., and Lv, R. (2022). Single-time Power Frequency Modulation and Peak -modulation Market Combined Clearing Method Considering New Energy Absorption Capacity. *IOP Conf. Ser. Earth Environ. Sci.* 1011, 012011. doi:10.1088/1755-1315/1011/1/012011

Liu, D., Jin, Z., Chen, H., Cao, H., Yuan, Y., Fan, Y., et al. (2021). Peak Shaving and Frequency Regulation Coordinated Output Optimization Based on Improving Economy of Energy Storage. *Electronics* 11 (1), 29. doi:10.3390/electronics11010029

Meng, G., Lu, Y., Liu, H., Ye, Y., Sun, Y., and Tan, W. (2021). Adaptive Droop Coefficient and Soc Equalization-Based Primary Frequency Modulation Control Strategy of Energy Storage. *Electronics* 10 (21), 2645. doi:10.3390/electronics10212645

Meng, L., Zafar, J., Shafiuzzaman, K., Collinson, A., Murchie, K. C., Coffele, F., et al. (2019). Fast Frequency Response from Energy Storage Systems—A Review of Grid Standards, Projects and Technical Issues. *IEEE Trans. smart grid* 11 (2), 1566. doi:10.1109/TSG.2019.2940173

Naseri, F., Karimi, S., Farjah, E., and Schaltz, E. (2021). *Supercapacitor Management System: A Comprehensive Review of Modeling, Estimation, Balancing, and Protection Techniques*. Renewable and Sustainable Energy Reviews, 2021.

Rancilio, G., Lucas, A., Kotsakis, E., Fulli, G., Merlo, M., Delfanti, M., et al. (2019). Modeling a Large-Scale Battery Energy Storage System for Power Grid Application Analysis. *Energies* 12 (17), 3312. doi:10.3390/en12173312

Saxena, A., and Shankar, R. (2022). Improved Load Frequency Control Considering Dynamic Demand Regulated Power System Integrating Renewable Sources and Hybrid Energy Storage System. *Sustain. Energy Technol. Assessments* 52, 102245. doi:10.1016/j.seta.2022.102245

Song, C., Feng, J., Yang, D., Zhou, B. W., and Qi, G. (2018). Collaborative Optimization of Integrated Energy Considering System Coupling. *Automation Electr. Power Syst.* 42 (10), 38. doi:10.7500/AEPS20170914008

Sun, B., He, X., Zhang, W., Li, Y., Gong, M., Yang, Y., et al. (2020). Control Strategies and Economic Analysis of an Lto Battery Energy Storage System for Agc Ancillary Service. *Energies* 13 (2), 505. doi:10.3390/en13020505

Wang, H., Wang, T., Xie, X., Ling, Z., Gao, G., and Dong, X. (2018). Optimal Capacity Configuration of a Hybrid Energy Storage System for an Isolated Microgrid Using Quantum-Behaved Particle Swarm Optimization. *Energies* 11 (2), 454. doi:10.3390/en11020454

Yang, N., Dong, Z., Wu, L., Zhang, L., Shen, X., Chen, D., et al. (2021). A Comprehensive Review of Security-Constrained Unit Commitment. *J. Mod. Power Syst. Clean Energy* 10 (3), 562–576. doi:10.35833/MPCE.2021.000255

Yang, N., Yang, C., Xing, C., Ye, D., Jia, J., Chen, D., et al. (2022). Deep Learning-based SCUC Decision-making: An Intelligent Data-driven Approach with Self-learning Capabilities. *IET Generation Trans Dist* 16 (4), 629–640. doi:10.1049/gtd2.12315

Yang, R. (2016). *Design And Optimization of Hybrid Energy Storage for Photovoltaic Power Fluctuation Smoothing Based on Frequency Analysis*. PhD Thesis. The University of Wisconsin-Milwaukee.

Ye, J., Zhao, D., Zhang, L., Li, Z., and Zhang, T. (2021). Research on Combined Electricity and Heating System Scheduling Method Considering Multi-Source Ring Heating Network. *Front. Energy Res.* 826, 906. doi:10.3389/fenrg.2021.800906

Zhang, F., Yang, Z., Wang, G., and Meng, K. (2018). "Control Strategy of Hybrid Energy Storage System to Improve Agc Performance of Thermal Generator," in *2018 IEEE Innovative Smart Grid Technologies-Asia (ISGT Asia)* (IEEE), 1299–1304. doi:10.1109/isgt-asia.2018.8467771

Zhang, L., Xie, Y., Ye, J., Xue, T., Cheng, J., Li, Z., et al. (2021). Intelligent Frequency Control Strategy Based on Reinforcement Learning of Multi-Objective Collaborative Reward Function. *Front. Energy Res.* 587, 760525. doi:10.3389/fenrg.2021.760525

Conflict of Interest: HH, HW, YC, XC, and TL were employed by Powerchina Hubei Electric Engineering Co., Ltd.

Publisher's Note: All claims expressed in this article are solely those of the authors and do not necessarily represent those of their affiliated organizations, or those of the publisher, the editors and the reviewers. Any product that may be evaluated in this article, or claim that may be made by its manufacturer, is not guaranteed or endorsed by the publisher.